ELSEVIER

Chemical Geology 175 (2001) 485–494

CHEMICAL GEOLOGY
INCLUDING
ISOTOPE GEOSCIENCE

www.elsevier.com/locate/chemgeo

An experimental study of forsterite dissolution rates as a function of temperature and aqueous Mg and Si concentrations

Eric H. Oelkers *

Laboratoire de Géochimie, CNRS / URM 5563, Université Paul Sabatier, 38 rue des Trente-six Ponts, 31400 Toulouse, France

Received 23 September 1999; accepted 27 June 2000

Abstract

Steady state forsterite dissolution rates, at far from equilibrium conditions and pH = 2 ± 0.04, were measured as a function of aqueous magnesium and silica concentrations, and temperatures from 25°C to 65°C. All rates were measured in mixed flow reactors and exhibited stoichiometric dissolution. Measured rates are found to be independent of both aqueous magnesium and silica concentrations. The temperature dependence of the pH 2 forsterite dissolution rates obtained in this study is consistent with an Arrhenius equation of the form

$$r = A_A \exp(-E_A/RT)$$

where r signifies the overall forsterite steady state dissolution rate, A_A refers to a pre-exponential factor equal to 0.190 mol cm^{-2} s^{-1}, E_A designates an activation energy equal to 63.8 kJ/mol, R represents the gas constant, and T denotes absolute temperature.

The observed variation of forsterite dissolution rates with aqueous composition is interpreted to originate from its dissolution mechanism. The forsterite structure consists of isolated silica tetrahedra that are branched together by magnesium octahedra chains. Mg–O bonds apparently break more rapidly than Si–O bonds in this structure. The breaking of octahedra chain linking Mg–O bonds, which is apparently catalyzed by hydrogen ion adsorption at acidic conditions, leads directly to the destruction of the mineral. As the rate-controlling precursor complex for this mineral is formed by a hydrogen adsorption reaction, forsterite dissolution rates are unaffected by aqueous Mg and Si activities.

Keywords: Forsterite dissolution rates; Arrhenius equation; Activation energy, dissolution mechanisms

1. Introduction

The motivation for this study is the improved understanding of the dissolution rates and mechanism of the silicate minerals. Towards this goal, a significant number of studies have been focused over the past several years on characterizing aluminosilicate dissolution rates as a function of chemical affinity and/or aqueous Al and Si activities (see for example, Nagy et al., 1991; Burch et al., 1993; Oelkers et al., 1994; Gautier et al., 1994; Oelkers and Schott, 1995a, 1999; Murphy et al., 1996; Devi-

* Tel.: +33-5-61-55-87-85; fax: +33-5-61-55-81-38.
E-mail address: oelkers@lucid.ups-tlse.fr (E.H. Oelkers).

0009-2541/01/$ - see front matter
PII: S0009-2541(00)00352-1

dal et al., 1997). Knowledge of dissolution rate variation of these minerals on the aqueous activities of their constituent metals leads to significant advances in the understanding of their dissolution mechanisms. In an attempt to generalize the results of these past studies to the magnesium silicates, far from equilibrium steady state dissolution rates of San Carlos forsterite were measured as a function of aqueous Mg and Si concentrations and temperature at pH = 2. The purpose of the present communication is to report the results of this experimental study and use them to illuminate the olivine dissolution mechanism.

This work builds upon the large number of forsterite dissolution studies that have been performed over the past 30 years (Luce et al., 1972; Sanemasa et al., 1972; Grandstaff, 1978, 1980; Murphy and Helgeson, 1987, 1989; Blum and Lasaga, 1988; Wogelius and Walther, 1991, 1992; Casey and Westrich, 1992; Chen and Brantley, 2000; Rosso and Rimstidt, 2000; Pokrovsky and Schott, 1999, 2000a,b). Blum and Lasaga (1988) reported that 25°C forsterite dissolution rates, determined from Si release, decrease with increasing pH in acidic conditions, but increase with increasing pH in basic conditions. Wogelius and Walther (1991, 1992) measured forsterite dissolution rates at 25°C and 65°C; these investigators observed that the pH dependence of their rates is independent of temperature and thus activation energies are pH independent. Oelkers (1999) presented a review and comparison of the dissolution rates and mechanisms of forsterite and enstatite; some of the data presented in this study are presented in the figures of that review. Chen and Brantley (2000) reported olivine dissolution rates at 65°C and four distinct solution pH. Care of these values, Chen and Brantley (2000) conclude that the activation energy of forsterite dissolution varies with pH. Rosso and Rimstidt (2000) used 772 measurements to determine forsterite dissolution rates at nine distinct temperature/pH points (25°C, 35°C, and 45°C; pH = 1.8, 2.8 and 3.8). These authors conclude that there is no variation of activation energy with pH. Pokrovsky and Schott (2000b) measured forsterite dissolution rates at 25°C at pH ranging from 1 to 12. These authors presented evidence that forsterite dissolution rates do not increase with increasing pH at basic conditions and suggest that the experiments reported by Blum and Lasaga (1988) had not attained steady state at basic conditions.

2. Theoretical background

The standard state adopted in this study is that of unit activity for pure minerals and H_2O at any temperature and pressure. For aqueous species other than H_2O, the standard state is unit activity of the species in a hypothetical 1 molal solution referenced to infinite dilution at any temperature and pressure. All aqueous activities and equilibrium constants used in the present study were generated using EQ3NR (Wolery, 1983) and SUPCRT92 (Johnson et al., 1992), respectively.

The overall rate of a chemical reaction (r) can be considered to be the difference between the forward rate (r_+) and the reverse rate (r_-) such that

$$r = r_+ - r_- = r_+\left(1 - \frac{r_-}{r_+}\right) \tag{1}$$

It has been demonstrated with the aid of transition state theory, that this second term, which accounts for the effects of inverse reaction, can be expressed as (Aagaard and Helgeson, 1977, 1982; Lasaga, 1981; Helgeson et al., 1984; Murphy and Helgeson, 1987)

$$\left(1 - \frac{r_-}{r_+}\right) = \left(1 - \exp(-A/\sigma RT)\right) \tag{2}$$

where A refers to the chemical affinity of the overall reaction, σ stands for Temkin's average stoichiometric number equal to the ratio of the rate of destruction of the activated or precursor complex relative to the overall rate, R designates the gas constant, and T represents absolute temperature. All dissolution rates measured in the present study were performed at far from equilibrium conditions, such that $A \gg \sigma RT$. At these conditions $r_- \ll r_+$ and thus $r \approx r_+$.

For the case of mineral dissolution reactions, r_+ can be assumed to be proportional to the concentration of a rate-controlling precursor complex at the mineral surface in accord with (Wieland et al., 1988; Oelkers et al., 1994):

$$r_+ = k_+[\mathrm{P}^{\cdot}], \tag{3}$$

where k_+ refers to a rate constant consistent with the $\mathrm{P}^{\cdot}$ precursor complex and $[\mathrm{P}^{\cdot}]$ stands for its

concentration. The precursor complex is assumed to be in equilibrium with the reactants and therefore the variation of its concentration with aqueous solution composition can be deduced from the law of mass action for the reaction forming this complex from the original mineral.

Two general types of precursor forming reactions have been observed for the silicate minerals (Oelkers and Schott, 1995b; Oelkers, 1996): (1) simple absorption reactions and (2) metal–proton exchange reactions. Minerals whose rate-controlling precursor complexes form by simple absorption reactions include those whose dissolution requires the breaking of only one type of cation–oxygen bond. Examples of these minerals are single (hydr)oxides (e.g. gibbsite, Nagy and Lasaga, 1992; and quartz, Berger et al., 1994) and some multi-oxide silicates (e.g. anorthite, Oelkers and Schott, 1995a). Because their rate-controlling precursor complexes are formed by simple absorption reactions, the concentration of these complexes and thus r_+ are independent of the aqueous concentration of the metals comprising the mineral. A reaction forming a rate-controlling precursor complex by hydrogen ion adsorption can be written

$$n_4\mathrm{H}^+ + > \mathrm{M{-}OH} = \mathrm{P}^{\cdot} \tag{4}$$

where $> \mathrm{M{-}OH}$ represents a potentially reactive surface site, and n_4 stands for a stoichiometric coefficient equal to the number of hydrogen ions that need to be absorbed to create one precursor complex. Combining the law of mass action for reaction (4) with Eq. (3) and the fact that there are a limited number of reactive sites on the mineral surface leads to (Oelkers, 1996):

$$r_+ = k_+\left[\mathrm{P}^{\cdot}\right] = k_+\left(\frac{K_4^{\cdot} a_{\mathrm{H}^+}^{n_4}}{1 + K_4^{\cdot} a_{\mathrm{H}^+}^{n_4}}\right) \tag{5}$$

where $K_4^{\cdot}$ designates the equilibrium constant for reaction (4) and a_i denotes the activity of the subscripted aqueous species. Eq. (5) reduces to

$$r_+ = k_+ K_4^{\cdot} a_{\mathrm{H}^+}^{n_4} \tag{6}$$

when the surface contains relatively few precursor complexes ($K_4^{\cdot} a_{\mathrm{H}^+}^{n_4} \ll 1$).

Minerals, whose rate-controlling precursor complex is formed by metal–proton exchange reactions, include those multi-oxides whose dissolution requires the breaking of several different cation–oxide bond types. Evidence suggests that these metal–proton exchange reactions lead to formation of neutrally charged precursor complexes in a variety of minerals (see Chou and Wollast, 1984, 1985; Sverdrup and Warfvinge, 1993, 1995; Oelkers, 1996; Oelkers and Schott, 1998). These exchange reactions invoke the breaking of the more reactive cation–oxygen bonds that are not essential to the structure, thus better exposing to hydrolysis the bonds essential to the structure. Examples of minerals following this type of reaction mechanism include albite (Oelkers et al., 1994), K-feldspar (Gautier et al., 1994), kaolinite (Devidal, 1994, 1997), kyanite (Oelkers and Schott, 1994, 1999), analcime (Murphy et al., 1996), heulandite (Ragnarsdottir, 1993; Ragnarsdottir et al., 1996), and the pyroxenes (Oelkers, 1999). For the case where a neutrally charged precursor complex is formed by the exchange of one type of metal cation, the precursor complex forming reaction can be expressed as

$$z \cdot n_7\mathrm{H}^+ + > \mathrm{M{-}OH} = \mathrm{P}^{\cdot} + n_7\mathrm{M}^z \tag{7}$$

where n_7 stands for a stoichiometric coefficient equal to the number of cations that need to be removed from the mineral structure to create one precursor complex, M denotes the exchanged metal, and z designates its valence. Combining the law of mass action for exchange reaction (7) with Eq. (3) leads to (Oelkers, 1996):

$$r_+ = k_+\left[\mathrm{P}^{\cdot}\right] = k_+\left(\frac{K_7^{\cdot}\left(\dfrac{a_{\mathrm{H}^+}^z}{a_{\mathrm{M}^z}}\right)^{n_7}}{1 + K_7^{\cdot}\left(\dfrac{a_{\mathrm{H}^+}^z}{a_{\mathrm{M}^z}}\right)^{n_7}}\right) \tag{8}$$

where $K_7^{\cdot}$ designates the equilibrium constant for reaction (7). Eq. (8) reduces to

$$r_+ = k_+ K_7^{\cdot}\left(\frac{a_{\mathrm{H}^+}^z}{a_{\mathrm{M}^z}}\right)^{n_7} \tag{9}$$

when the surface contains relatively few precursor complexes

$$\left(K_7^{\cdot}\left(\frac{a_{\mathrm{H}^+}^z}{a_{\mathrm{M}^z}}\right)^{n_7} \ll 1\right).$$

Because the chemical affinity for the overall dissolution reaction depends on the aqueous concentration of its constituent metals, the overall dissolution rate of these minerals will appear to depend on chemical affinity at far from equilibrium conditions (see Schott and Oelkers, 1995).

The forsterite structure consists of individual silicon–oxygen tetrahedra linked by magnesium atoms, each of which is in octahedral coordination. A major structural feature of forsterite is the existence of serrated Mg octahedra chains that run parallel to the *z*-axis (see Brown, 1980). It follows that the dissolution mechanism of forsterite will depend greatly on the relative reaction rates of the various Mg–O and Si–O bonds in the mineral structure. If either the Si–O bonds or the Mg–O bonds adjoining Si atoms break faster during dissociation than the octahedral chain linking Mg–O bonds in this structure, Si could be liberated through exchange reactions, without destroying the mineral structure, resulting in partially detached Mg octahedra. As partially detached Mg octahedra detach from the mineral structure faster than fully attached Mg octahedra, the former would constitute the rate limiting precursor complex for the overall dissolution reaction. If this were the case, forsterite dissolution would be consistent with Eqs. (7)–(9) and depend on aqueous silica concentration at far from equilibrium conditions. In contrast, if the octahedral chain linking Mg–O bonds break more rapidly than either the Si–O bonds or the Mg–O bonds adjoining Si atoms in the olivine structure, the breaking of the Mg octahedral chain would liberate the individual Si tetrahedra, completely dissolving the mineral. Far from equilibrium forsterite dissolution rates would be independent of both aqueous Si and Mg concentration. Assessment of the variation with solution composition of forsterite dissolution rates obtained in the present study will enable deduction of the relative rates of bond breaking in the olivine structure, as well as providing insight into this mineral's dissolution mechanism.

3. Material preparation and experimental methods

Natural San Carlos forsterite crystals, having an average size of ~ 0.5 cm were obtained from Wards Natural Science. The crystals were handpicked then ground with an agate mortar and pestle. The size fraction between 50 and 100 μm was obtained by sieving. This fraction was cleaned ultrasonically using acetone to remove fine particles, rinsed with distilled water, and dried overnight at 80°C. The specific surface area of the cleaned powder is 808 ± 80 cm^2/gm as determined by krypton adsorption using the BET method. X-ray diffraction (XRD) of this powder indicates that the material is essentially pure olivine. The chemical composition, determined by electron microprobe, indicates this forsterite has an average composition of $(Mg_{1.78}Fe_{0.17})Si_{1.00}O_4$ when normalized to four oxygens. All dissolution experiments were performed in mixed flow reactors. The ground forsterite was placed in 250 ml Azlon plastic reactors, which were continuously stirred with floating Teflon stirring bars. These reactors were immersed in a water bath held at a constant temperature ± 1°C. Fluid is injected into this reactor using a Gilson peristaltic pump, which allows fluid flow rates from 0.05 to 10 g/min. The solution left the reactor through a 0.45-μm Teflon filter. The inlet fluid for all experiments was stored in a compressible, sealed polyethylene container during the experiments. Neither reactor corrosion nor secondary phase precipitation was observed visually or by optical microscopy during any of the experiments.

These reactor systems are ideally suited to investigate water/mineral reaction rates. The fluid saturation state and composition can be regulated by either changing the flow rate or the input solution composition without dismantling the reactor and/or changing the amount of mineral present during the experiment. A steady state dissolution rate, as indicated by constant outlet Mg and Si concentration, was obtained after an elapsed time ranging from 2 h to 1 day, depending on the flow rate. Dissolution experiments were carried out in fluids comprised of demineralized/degassed H_2O, Merck reagent grade HCl and $MgCl_2$, and H_4SiO_4(aq) obtained from the dissolution of amorphous silica for 1 week at 90°C. Reactive fluid magnesium and iron concentrations were determined using atomic absorption spectroscopy (Perkin Elmer Zeeman 5000); silica concentrations were measured using the Molybdate Blue method (Koroleff, 1976). The reproducibility of chemical analyses were $\pm 4\%$. Outlet fluid pH was

measured immediately after sampling. The pH of all outlet solutions measured at 25°C was 2.00 ± 0.04. Species distribution calculations indicate that these values differ by less than 0.02 pH units from the corresponding true values at the experimental temperature. Outlet solutions were undersaturated with respect to all possible secondary phases other than in several cases SiO_2(s). No SiO_2 was observed to precipitate during the experiments, and the relative release rate of Mg vs. Si during the experiments is consistent with the stoichiometric dissolution of forsterite without secondary phase precipitation.

4. Experimental results and discussion

Steady state dissolution rates (r) were computed from the measured solution compositions using

$$r = \frac{\Delta c_i F}{\nu_1 s} \tag{10}$$

where Δc_i stands for the concentration difference between the inlet and outlet of the ith element in solution, F represents the fluid flow rate, ν_i refers to the stoichiometric number of moles of the ith element in one mole of the forsterite, and s denotes the total mineral surface area present in the reactor. Resulting dissolution rates, together with inlet and outlet total magnesium and silica concentrations for all experiments are listed in Tables 1 and 2. The surface areas used to calculate these rates were that measured on the fresh (unreacted) mineral powder. Repeated runs performed using these powdered mineral samples indicate that these surface areas did not vary by more than $\sim 15\%$ during the experiments. The chemical affinity with respect to forsterite dissolution of all solutions considered in Tables 1 and 2 range from 38 to 45 kJ/mol.

An example of the temporal chemical evolution of the fluid during an experiment is illustrated in Fig. 1a. It can be seen in this figure that the aqueous Mg and Si concentrations in the reactor increase systematically with time attaining a steady state concentration after ~ 200 min of elapsed time. The temporal evolution of the Mg/Si ratio of these reactive aque-

Table 1
Experimental conditions and results of steady state dissolution measurements of San Carlos forsterite performed at 25°C and pH = 2 in the present study

Experiment number	Surface area (cm^2)	Flow rate (g/min)	Input Si (mol/kg $\times 10^5$)	Input Mg (mol/kg $\times 10^5$)	Outlet Si (mol/kg $\times 10^5$)	Outlet Mg (mol/kg $\times 10^5$)	Rate (mol cm^{-2} $s^{-1} \times 10^{12}$)
OL2-08	1483	3.28	0.00	0.00	4.25	8.23	1.57
OL2-10	1483	1.20	0.00	0.00	13.10	25.00	1.76
OL2-12	1483	8.55	0.00	0.00	1.26	2.38	1.21
OL2-13	1483	0.43	0.00	0.00	25.21	47.15	1.23
OL3-15	570	2.00	0.00	0.00	2.41	4.33	1.41
OL3-16	570	1.21	0.00	0.00	4.39	12.10	1.55
OL3-19	570	0.56	0.00	0.00	6.40	15.20	1.05
OL4-01	1019	1.08	0.00	100.00	7.58	115.00	1.33
OL4-02	1019	0.44	0.00	100.00	18.37	136.00	1.33
OL4-03	1019	0.78	0.00	100.00	9.90	120.00	1.27
OL4-04	1019	3.20	0.00	100.00	2.47	105.00	1.29
OL4-05	1019	1.23	0.00	100.00	5.98	112.00	1.21
OL5-01	1669	1.19	45.79	0.00	56.34	19.10	1.25
OL5-02	1669	3.23	45.79	0.00	49.59	6.88	1.23
OL5-03	1669	0.80	45.79	0.00	62.66	30.50	1.34
OL5-04	1669	6.39	45.79	0.00	47.63	3.33	1.18
OL7-04	1223	3.34	0.00	50.00	2.69	54.80	1.22
OL7-05	1223	0.74	0.00	50.00	11.63	70.40	1.17
OL7-06	1223	1.53	0.00	50.00	6.22	61.30	1.30
OL8-03	1432	3.23	22.72	0.00	25.47	6.44	1.03
OL8-05	1432	0.82	22.72	0.00	36.27	23.40	1.29
OL8-08	1432	1.64	22.72	0.00	29.03	11.20	1.20

Table 2
Experimental conditions and results of steady state dissolution measurements of San Carlos forsterite performed pH = 2 and temperatures other than 25°C in the present study

Experiment number	Temperature (°C)	Surface area (cm^2)	Flow rate (g/min)	Outlet Si (mol/kg × 10^5)	Outlet Mg (mol/kg × 10^5)	Rate (mol cm^{-2} s^{-1} × 10^{12})
OL1-04	45	772	1.25	34.59	72.46	9.36
OL6-01	65	922	1.74	85.84	168.00	27.03
OL6-02	55	922	1.98	30.01	55.00	10.74
OL6-03	35	922	1.93	7.61	14.90	2.65

ous fluids are given in Fig. 1b. The reactive fluids of this experiment were Mg and Si-free prior to the placing of the solid into the reactor, and thus all Mg and Si in solution originates from the reacting forsterite. An initial preferential Mg release is apparent; after ~120 min of elapsed time, the Mg/Si ratio of the reactive fluid decreases and becomes equal to that of the dissolving forsterite, consistent with stoichiometric dissolution. The quantity of initial preferential Mg or Si release apparently depends on fluid composition; Si is found to be preferentially released in high pH solutions (Pokrovsky and Schott, 2000b). In either case this initial non-stoichiometric preferential release is rapid and likely stems from the equilibration with solution of Si and Mg present near the surface of the original ground, cleaned, and dried forsterite powder used in these dissolution experiments. This initial preferential Mg release at acid conditions was interpreted by Pokrovsky and Schott (1999) to stem from a Mg for proton exchange reaction limited to the first several molecular layers of the forsterite.

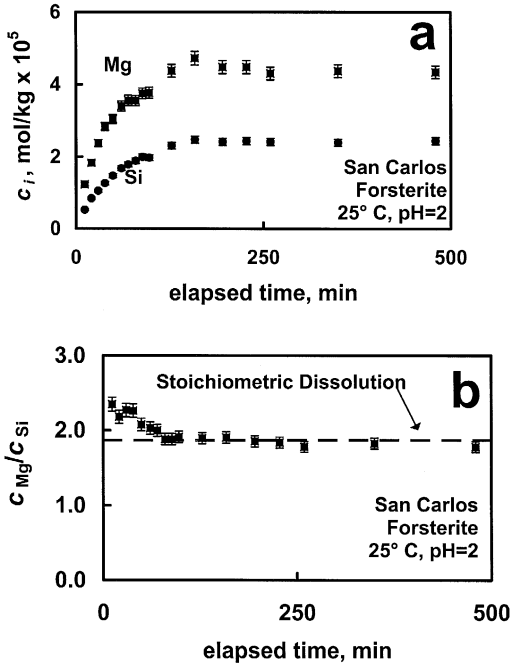

Fig. 1. Temporal evolution of outlet solution composition during experiment OL3-15: (a) outlet solution Mg and Si concentrations (c_{Mg} and c_{Si}) and (b) the ratio of these concentrations. The symbols represent measured solution compositions; the error bars surrounding these points correspond to a 4% uncertainty in c_{Mg} and c_{Si}. The dashed line corresponds to the Mg/Si ratio of the dissolving forsterite.

The difference between inlet and outlet Mg concentrations for all steady state experiments is depicted as a function of the corresponding Si concentration change in Fig. 2. The solid line in this figure corresponds to the Mg/Si ratio of the dissolving forsterite. It can be seen in this figure that steady state forsterite dissolution is essentially stoichiometric. Outlet Fe concentrations were only obtained for outlet solutions of the OL8 experimental series. Measured Fe concentrations were found to be within ±10% of those estimated, assuming stoichiometric dissolution.

Measured forsterite forward dissolution rates at 25°C are illustrated as a function of aqueous Si and Mg activities in Fig. 3. Measured constant temperature forsterite dissolution rates appear to be independent of aqueous Mg and Si activities. These observations imply that although there may be a rapid initial Mg for proton exchange reaction occurring on the forsterite surface, this reaction does not form the rate-controlling precursor complex. At acidic conditions forsterite rates decrease with decreasing hydro-

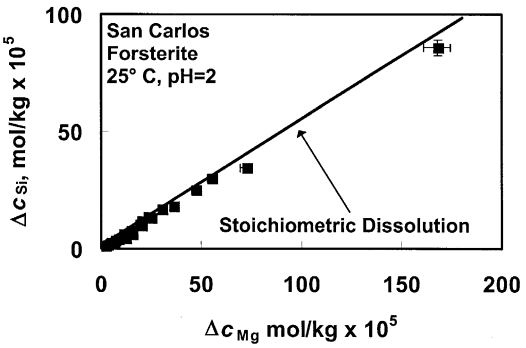

Fig. 2. The difference between steady state inlet and outlet solutions Mg concentration as a function of the corresponding difference between inlet and outlet solution Si concentrations (Δc_{Mg} and Δc_{Si}, respectively). The symbols represent measured solution compositions; the error bars surrounding these points correspond to a 4% uncertainty in Δc_{Mg} and Δc_{Si}. The solid line corresponds to the Mg/Si ratio of the dissolving forsterite.

gen ion activity (Blum and Lasaga, 1988; Wogelius and Walther, 1991; Chen and Brantley, 2000; Rosso and Rimstidt, 2000; Pokrovsky and Schott, 2000b). It seems likely therefore that forsterite dissolution is controlled by a precursor complex formed by a protonation reaction consistent with reaction (4); this protonation reaction tends to weaken adjacent octahedral chain linking Mg–O bonds in the mineral structure. The breaking of these Mg–O bonds is slow relative to the protonation reaction and results in the simultaneous liberation of magnesium and silicon from the forsterite structure. Simultaneous Mg and Si liberation during forsterite dissolution is consistent with the lack of extensive leached layer formation on forsterite surfaces (Schott and Berner, 1985) and on other similarly structured orthosilicates (Westrich et al., 1993). It should be noted however that Pokrovsky and Schott (2000b) observed a dependence of forsterite dissolution rates on aqueous Si concentration at basic conditions. This was interpreted to stem from Si exchange reactions promoted by the relative fast breaking of the Mg–O bonds adjoining the Si atoms in the forsterite structure.

The variation of mineral dissolution rates with temperature is commonly described using the empirical Arrhenius equation given by

$$r_+ = A_A \exp\left(\frac{-E_A}{RT}\right) \tag{11}$$

where A_A designates a pre-exponential factor and E_A refers to the activation energy defined by

$$E_A = -2.303R\left(\frac{\partial \log r_+}{\partial\left(\frac{1}{T}\right)}\right)_{pH} \tag{12}$$

An Arrhenius plot depicting the logarithm of measured forsterite dissolution rates as a function of reciprocal temperature is illustrated in Fig. 4. Taking account of Eq. (12), it follows that the slopes of the lines drawn through the symbols in Fig. 4 are equal to $-E_A/2.303R$. The straight line depicted in this figure corresponds to an activation energy at pH = 2 of 63.8 kJ/mol with 95% confidence limits of ± 17 kJ/mol. This activation energy is somewhat less than the 79 kJ/mol value reported by Wogelius and Walther (1992). A regression of the data reported in

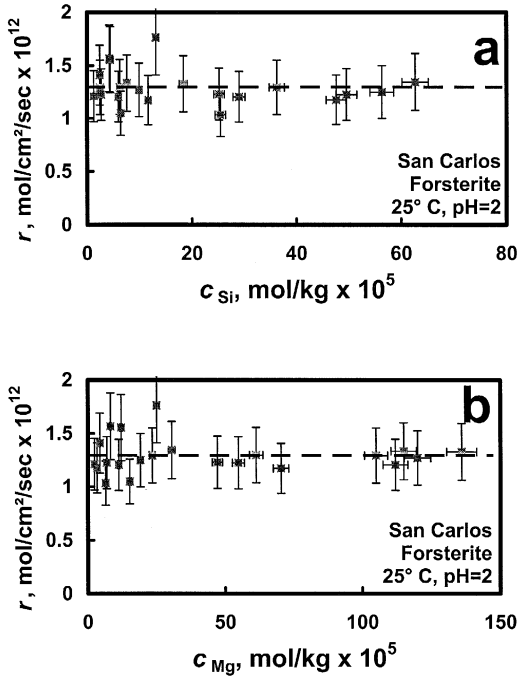

Fig. 3. Variation of the forsterite forward dissolution rates at pH = 2 and 25°C with aqueous (a) silicon and (b) magnesium concentrations. The symbols correspond to experimental data reported in Table 1, and the error bars correspond to a $\pm 20\%$ estimated uncertainty of these rates. The linear curve in there figures corresponds to a constant rate of 1.25×10^{-12} mol cm^{-2} s^{-1}.

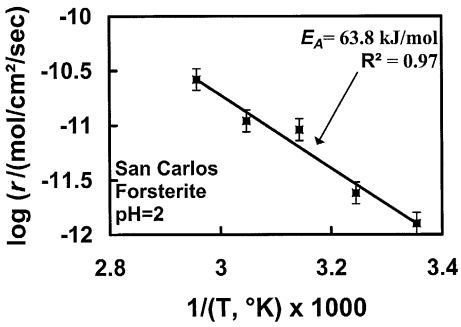

Fig. 4. Variation of the logarithm of forsterite forward dissolution rates as a function of 1000 times reciprocal temperature at pH = 2. The symbols represent data reported in Tables 1 and 2, and the error bars correspond to a ± 0.1 log unit estimated uncertainty of these data. The linear curve corresponds to a least squares fit of the data; the activation energy and coefficient of determination (R^2) of this curve are given in the figure.

this study together with those of Blum and Lasaga (1988) and Wogelius and Walther (1992) yields an activation energy of 75 kJ/mol (see Oelkers, 1999).

5. Experimental and computational uncertainties

Uncertainties associated with the rate constants generated above arise from a variety of sources, including the measurement of aqueous solution concentrations, fluid flow rates, and mineral surface areas. The uncertainties in the measured values of the total aqueous silica and magnesium concentrations are in the order of $\pm 4\%$ or less. Computational and experimental uncertainty in the pH of these solutions are in the order of ± 0.04 pH units. Uncertainties in fluid flow rate measurements are not more than 2%. In contrast, the uncertainties associated with the measurement of the surface area of the forsterite powder are $\pm 10\%$. In addition, the mineral surface area changed somewhat over the duration of each experiment. To assess the temporal effects of changing mineral surface areas on the resulting dissolution rates, one of the final fluid flow rates for several of the mineral samples of a single fluid composition was set approximately equal to the first. The difference in the resulting fluid concentrations was in the order of 15% or less. Because the uncertainties associated with the resulting forsterite dissolution rates are directly proportional to the uncertainties in the fluid concentrations and the mineral surface areas, the overall uncertainties in these rates are in the order of $\sim \pm 20\%$.

6. Conclusion

Forsterite dissolution rates measured at pH = 2 and at far from equilibrium conditions are found to be independent of aqueous Mg and Si concentrations; they are also in general agreement with corresponding rates previously reported in the literature. Forsterite dissolution in acidic conditions most likely proceeds via two major steps: (1) surface protonation, forming rate-controlling precursor complexes, followed by (2) the breaking of octahedra chain linking Mg–O bonds. Breaking these Mg–O bonds simultaneously liberates Mg and Si from the forsterite structure. This mechanism is manifested in forsterite forward dissolution rates that are independent of aqueous Mg and Si activities. The variation of forsterite dissolution rates with pH and comparison of these rates with computed forsterite surface speciation is reported by Pokrovsky and Schott (2000a,b). The rates and mechanisms of forsterite dissolution are compared with those of enstatite by Oelkers (1999).

Acknowledgements

I would like to thank Oleg Pokrovsky, Jacques Schott, Jean-Louis Dandurand, Robert Gout, Patrica Fournier, Carlos Jové, Jean-Marie Gautier, Marwan Alkattan, and Stacey Callahan for the helpful discussions during the course of this study. I would also like to thank Susan Brantley, Roy Wogelius, and Jichwar Ganor for providing enlightening reviews of an earlier version of this manuscript. Support from Centre National de la Recherche Scientifique is gratefully acknowledged.

References

Aagaard, P., Helgeson, H.C., 1977. Thermodynamic and kinetic constraints on the dissolution of feldspars. Geol. Soc. Am. 9, 873, Abstracts with Program.

Aagaard, P., Helgeson, H.C., 1982. Thermodynamic and kinetic constraints on reaction rates among minerals and aqueous

solutions: I. Theoretical considerations. Am. J. Sci. 282, 237–285.

Berger, G., Cadoré, E., Schott, J., Dove, P., 1994. Dissolution rate of quartz in Pb and Na electrolyte solutions. Effect of the nature of surface complexes and reaction affinity. Geochim. Cosmochim. Acta 58, 541–551.

Blum, A.E., Lasaga, A.C., 1988. Role of surface speciation in the low temperature dissolution of minerals. Nature 331, 431–433.

Brown, G.E., 1980. Olivines and silicate spinels. Rev. Miner. 5, 275–381.

Burch, T.E., Nagy, K.L., Lasaga, A.C., 1993. Free energy dependence of albite dissolution kinetics at 80°C. Chem. Geol. 105, 137–162.

Casey, W.H., Westrich, H.R., 1992. Control of dissolution rates of orthosilicate minerals by divalent metal–oxygen bonds. Nature 355, 157–159.

Chen, Y., Brantley, S.L., 2000. Forsterite dissolution at 65°C and $2 < pH < 5$. Chem. Geol. 165, 267–281.

Chou, L., Wollast, R., 1984. Study of the weathering of albite at room temperature and pressure with a fluidized bed reactor. Geochim. Cosmochim. Acta 48, 2205–2217.

Chou, L., Wollast, R., 1985. Steady state kinetics and dissolution mechanisms of albite. Am. J. Sci. 285, 963–993.

Devidal, J.L., 1994. Solubilité et cinétique de dissolution/précipitation de la kaolinite en milieu hydrothermal. Approche expérimentale et modélisation. PhD thesis, University Paul Sabatier, Toulouse, France.

Devidal, J.L., Schott, J., Dandurand, J.L., 1997. An experimental study of kaolinite dissolution and precipitation kinetics as a function of chemical affinity and solution composition at 150°C, 40 bars, and pH 2, 6.8, and 7.8. Geochim. Cosmochim. Acta 61, 5165–5186.

Gautier, J.-M., Oelkers, E.H., Schott, J., 1994. Experimental study of K-feldspar dissolution rates as a function of chemical affinity at 150°C and pH 9. Geochim. Cosmochim. Acta 58, 4549–4560.

Grandstaff, D.E., 1978. Changes in surface area and morphology and the mechanism of forsterite dissolution. Geochim. Cosmochim. Acta 42, 1899–1901.

Grandstaff, D.E., 1980. The dissolution of forsteritic olivine from Hawaiian beach sand. Proc., 3rd Int. Symp. Water–Rock Interact, pp. 72–74.

Helgeson, H.C., Murphy, W.M., Aagaard, P., 1984. Thermodynamic and kinetic constraints on reaction rates among minerals and aqueous solutions: II. Rate constants, effective surface area, and the hydrolysis of feldspar. Geochim. Cosmochim. Acta 48, 2405–2432.

Johnson, J.W., Oelkers, E.H., Helgeson, H.C., 1992. SUPCRT92: a software package for calculating the standard molal properties of minerals gases, aqueous species and reactions among them from 1 to 5000 bars and 0 to 1000°C. Comp. Geosci. 18, 899–947.

Koroleff, F., 1976. Determination of silicon. In: Grasshoff, K. (Ed.), Methods of Seawater Analysis. Springer Verlag, New York, pp. 149–158.

Lasaga, A.C., 1981. Transition state theory. Rev. Miner. 8, 135–169.

Luce, R.W., Bartlett, R.W., Parks, G.A., 1972. Dissolution kinetics of magnesium silicates. Geochim. Cosmochim. Acta 36, 35–50.

Murphy, W.M., Helgeson, H.C., 1987. Thermodynamic and kinetic constraints on reaction rates among minerals and aqueous solutions: III. Activated complexes and the pH-dependence of the rates of feldspar, pyroxene, wollastonite, and olivine hydrolysis. Geochim. Cosmochim. Acta 51, 3137–3153.

Murphy, W.M., Helgeson, H.C., 1989. Thermodynamic and kinetic constraints on reaction rates among minerals and aqueous solutions: IV. Retrevial of rate constants and activation parameters for the hydrolysis of pyroxene, wollastonite, olivine, analusite and quartz. Am. J. Sci. 288, 17–101.

Murphy, W.M., Pabalan, R.T., Prikryl, J.D., Goulet, C.J., 1996. Reaction kinetics and thermodynamics of aqueous dissolution and growth of analcime and Na-clinoptilolite at 25°C. Am. J. Sci. 296, 128–186.

Nagy, K.L., Blum, A.E., Lasaga, A.C., 1991. Dissolution and precipitation kinetics of kaolinite at 80° and pH 3: The dependence on solution saturation state. Am. J. Sci. 291, 649–686.

Nagy, K.L., Lasaga, A.C., 1992. Dissolution and precipitation kinetics of gibbsite at 80°C and pH 3: The dependence on solution saturation state. Geochim. Cosmochim. Acta 56, 3093–3111.

Oelkers, E.H., 1996. Summary and review of the physical and chemical properties of rocks and fluids. Rev. Miner. 34, 131–191.

Oelkers, E.H., 1999. A comparison of enstatite and forsterite dissolution rates and mechanisms. In: Jamtveit, B., Meakin, P. (Eds.), Growth, Dissolution and Pattern Formation in Geosystems. Kluwer Academic Publishing, Dordrecht, pp. 253–268.

Oelkers, E.H., Schott, J., Devidal, J.L., 1994. The effect of aluminum, pH, and chemical affinity on the rates of aluminosilicate dissolution reactions. Geochim. Cosmochim. Acta 58, 2011–2024.

Oelkers, E.H., Schott, J., 1994. Experimental study of kyanite dissolution rates as a function of Al and Si concentration. Miner. Mag. 58A, 659–660.

Oelkers, E.H., Schott, J., 1995a. Experimental study of anorthite dissolution and the relative mechanism of feldspar hydrolysis. Geochim, Cosmochim. Acta 59, 5039–5053.

Oelkers, E.H., Schott, J., 1995b. The dependence of silicate dissolution rates on their structure and composition. In: Kharaka, Y.K., Chudaev, O.V. (Eds.), Water Rock Interaction. A.A. Balkema, Rotterdam, pp. 153–156.

Oelkers, E.H., Schott, J., 1998. Does organic acid adsorption effect alkali feldspar dissolution rates? Chem. Geol. 151, 235–246.

Oelkers, E.H., Schott, J., 1999. An experimental study of the dissolution rate of kyanite as a function of chemical affinity and solution composition. Geochim. Cosmochim. Acta 63, 785–798.

Pokrovsky, O., Schott, J., 1999. Olivine surface speciation and reactivity in aquatic systems. In: Armannsson, H. (Ed.), Geochemistry of the Earth's Surface. Balkema, Rotterdam, pp. 461–463.

Pokrovsky, O., Schott, J., 2000a. Forsterite surface composition in aqueous solutions: a combined potentiometric, electrokinetic, and spectroscopic approach. Geochim. Cosmochim. Acta (in press).

Pokrovsky, O., Schott, J., 2000b. Kinetics and mechanism of forsterite dissolution at 25°C and pH from 1 to 12. Geochim. Cosmochim. Acta (in press).

Ragnarsdottir, K.V., 1993. Dissolution kinetics of heulandite at pH 2–12 and 25°C. Geochim. Cosmochim. Acta 57, 2439–2449.

Ragnarsdottir, K.V., Graham, C.M., Allen, G.C., 1996. Surface chemistry of reacted heulandite determined by SIMS and XPS. Chem. Geol. 131, 167–181.

Rosso, J.J., Rimstidt, J.D., 2000. A high resolution study of forsterite dissolution rates. Geochim. Cosmochim. Acta 64, 797–811.

Sanemasa, I., Yoshida, L., Ozawa, T., 1972. The dissolution of olivine in aqueous solutions of inorganic acids. Bull. Chem. Soc. Jpn. 45, 1741–1746.

Schott, J., Berner, R.A., 1985. Dissolution mechanisms of pyroxenes and olivines during weathering. In: Drever, J.I. (Ed.), The Chemistry of Weathering. NATO ASI Ser., Ser. C: Math. Phys. Sci., vol. 149, pp. 35–53.

Schott, J., Oelkers, E.H., 1995. Dissolution and crystallization rates of silicate minerals as a function of chemical affinity. Pure Appl. Chem. 67, 603–610.

Sverdrup, H., Warfvinge, P., 1993. Calculating field weathering rates using a mechanistic geochemical model — PROFILE. J. Appl. Geochem. 8, 273–283.

Sverdrup, H., Warfvinge, P., 1995. Estimating field weathering rates using laboratory kinetics. Rev. Miner. 31, 485–541.

Westrich, H.R., Cygan, R.T., Casey, W.H., Zemitis, C., Arnold, G.W., 1993. The dissolution kinetics of mixed cation orthosilicate minerals. Am. J. Sci. 293, 869–893.

Wieland, E., Werhli, B., Stumm, W., 1988. The coordination chemistry of weathering: III. A potential generalization on dissolution rates of minerals. Geochim. Cosmochim. Acta 52, 1969–1981.

Wogelius, R.A., Walther, J.V., 1991. Olivine dissolution at 25°C: effects of pH, CO_2 and organic acids. Geochim. Cosmochim. Acta 55, 943–954.

Wogelius, R.A., Walther, J.V., 1992. Olivine dissolution at near-surface conditions. Chem. Geol. 97, 101–112.

Wolery, T.J., 1983. EQ3NR, a computer program for geochemical aqueous speciation–solubility calculations: users guide and documentation, UCRL-53414. Lawrence Livermore National Laboratory, Livermore, CA.